

# The facade system with ventilated channels for thermal insulation of newly constructed and renovated buildings



M.I. Nizovtsev<sup>a,\*</sup>, V.T. Belyi<sup>b</sup>, A.N. Sterlygov<sup>a</sup>

<sup>a</sup> Laboratory Problems of Energy Savings, Institute of Thermophysics, Russian Academy of Science, Siberian Branch, 1 Lavrent'ev Avenue, Novosibirsk 630090, Russia

<sup>b</sup> Thermoland Ltd., 38, Stantsionnaya Street, Apt. 5, Novosibirsk, Russia

## ARTICLE INFO

### Article history:

Received 4 March 2013

Received in revised form 29 January 2014

Accepted 1 February 2014

### Keywords:

Ventilated facade

Heat-insulating panel

Ventilated channels

Brick wall

Moisture analysis

## ABSTRACT

In the present paper, we describe a new thermal-insulating facade system for newly constructed and renovated buildings, based on heat-insulating panels with ventilated channels. The calculated data on thermal resistances of heat-insulating panels and on the reduced thermal resistances of brick walls with an external facade system, formed by the panels with ventilated channels, are reported as a function of panel thickness. Heat transfer performance uniformity factors of brick walls with different numbers of anchors used for mounting a panel on the brick wall are determined. The calculations show that the heat transfer performance uniformity factors of ventilated panels can be substantially increased in comparison with similar factors for traditional ventilated facade systems. Non-stationary thermal and moisture calculations of newly constructed and renovated buildings with brick outer walls were carried out to determine the humidity dynamics of heat-insulating and structural wall layers over a period of three years. The calculations prove that the examined configuration of ventilated channels is capable of providing for low moisture content and good heat-insulating properties of the walls. Photos and thermograms of building facades, thermally insulated with ventilated channels, are presented.

© 2014 Elsevier B.V. All rights reserved.

## 1. Introduction

In recent years, ventilated facade systems have found widespread use in various climatic zones due to their high energy performance, rich variety of available design solutions, reduced effect of solar radiation on indoor microclimate, good noise reduction properties, and possibility of rapid building repair and reconstruction [1].

Performance characteristics of ventilated facades are influenced by the outdoor conditions (the solar irradiance, the wind direction and speed, and the outdoor air temperature), and also by the indoor conditions (the temperature and humidity of the indoor air) and facade design features (air interlayer configuration, composition of used materials and their layout) [2].

In recent years, the wide use of ventilated facades in civil engineering and involvement of many factors, affecting the performance of such facades, stimulated numerous simulation studies aimed at gas dynamics and heat–mass transfer analysis of ventilated facades [3–6]. Fundamentals of free–convection flows, moving

along vertical surfaces under heating or cooling, were laid down in the classical works by Bar-Cohen and Rohsenow [7], Rohsenow et al. [8], and Sparrow et al. [9].

It should be noted, however, that, in spite of the permanently increasing number of numerical studies of ventilated facades, the development of valid engineering procedures for simulating such facade systems still remains an urgent problem. This is why of much significance are also experimental studies of ventilated facades, aimed at verification and optimization of simulation procedures [10–12].

In recently reported studies, special attention was paid to several design features of ventilated facades. For instance, it was noted in [13] that, although the external skin can play an important role in a facade system, the choice of external-skin material for ventilated facades was previously given insufficient attention. In [14], results of the study of the effect of a heat-reflecting film, provided on the surface of ventilated air cavity, were described; and the high performance of the film, especially at night in the winter season was shown. In [15], attention was drawn to the necessity of taking the building envelope mass into account while analyzing the performance of ventilated facades.

The literature also contains the results gained in the studies of performance characteristics of various “active” facades with forced

\* Corresponding author. Tel.: +7 383 316 53 36; fax: +7 383 316 53 36.  
E-mail address: [nizovtsev@itp.nsc.ru](mailto:nizovtsev@itp.nsc.ru) (M.I. Nizovtsev).

## Nomenclature

$d$	panel thickness (mm)
$D$	effective moisture diffusivity ( $\text{m}^2/\text{s}$ )
$H$	enthalpy of the humid material (J/kg)
$h$	phase-transition heat (J/kg)
$k$	absorption coefficient for solar radiation
$n$	number of mounting anchors per panel
$P$	water-vapor pressure (Pa)
$R$	thermal resistance, reduced resistance to the transfer of heat ( $\text{K m}^2/\text{W}$ )
$r$	heat transfer performance uniformity factors of the anchored panel
$t$	temperature ( $^{\circ}\text{C}$ )
$W_V$	volume humidity ( $\text{kg}/\text{m}^3$ )
$W$	relative mass humidity
$x, y$	coordinates (m)
$q_t$	heat-flux density ( $\text{W}/\text{m}^2$ )
$q_m$	moisture flux density ( $\text{kg}/\text{m}^2 \text{ s}$ )
$q_s$	incident flux of solar radiation ( $\text{W}/\text{m}^2$ )

### Greek symbols

$\tau$	time (s)
$\varphi$	relative humidity
$\mu$	vapor permeability coefficient ( $\text{kg}/\text{m s Pa}$ )
$\alpha$	heat-transfer coefficient ( $\text{W}/\text{m}^2 \text{ K}$ )
$\beta$	mass-transfer coefficient ( $\text{kg}/\text{m}^2 \text{ s Pa}$ )
$\lambda$	thermal conductivity ( $\text{W}/\text{m K}$ )

### Subscripts

air	air
$b$	boundary
$o$	structural layer
$p$	panel
red	reduced quantity
req	required value
req <sup>+</sup>	reduced value with allowance for anchors
sat	saturated water vapor

ventilation and adjustable shading elements [16] or with solar batteries, installed on the external surface [17,18].

In hot-climate regions, ventilated facades allow diminishing the influence of heating of external building-wall surfaces on the indoor microclimate [2,19]. Since the thermal-insulating properties of mineral wool heat-insulating materials are largely defined by the moisture state of the materials, in the region with low winter temperatures and with a long cold period, one of the main functions of ventilated facades is maintaining the outer heat-insulation layer in a dry state [20].

In ventilated facades with a heat-insulation layer, various materials were used; nonetheless, as a rule, such facades normally feature a design common to all such facades. During installation of a ventilated facade on a building wall, an intersystem formed by metal outriggers and supporting profiles is first mounted. Then, at a certain distance from the heat-insulation layer, an external-skin layer is to be installed. Thus, in installation of a standard ventilated facade, all operations are performed on the construction site; this circumstance makes the inspection of work quality difficult and prolongs the time necessary for the mounting.

In the present article, we describe a new facade system based on factory-produced heat-insulating panels with ventilated channels and report results of thermal and moisture calculations, performed for brick walls of newly constructed and renovated buildings, provided with the new facade system.

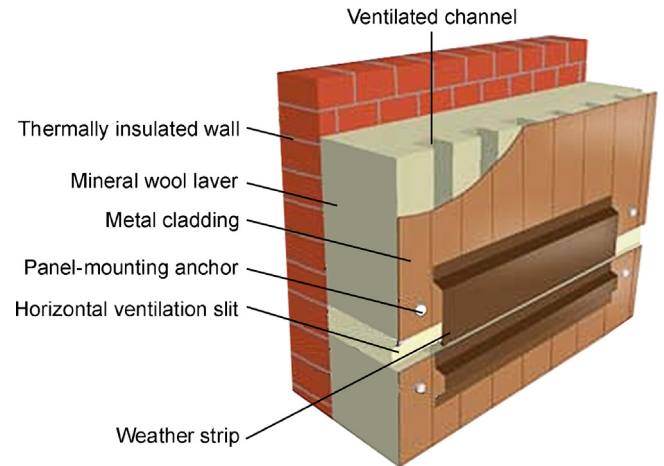


Fig. 1. The facade system with ventilated channels.

## 2. The facade system with ventilated channels

Developing the new facade system, we intended to design a high prefabrication system, suitable for thermal insulation of building walls in both newly constructed and renovated buildings. Such a facade system with ventilated panels was developed. The new facade system (see Fig. 1) is based on heat-insulating panels admitting their line production at factories [21]. From the outside, each panel is provided with a thin metal cladding, covered with a special decorative coating. The cladding is glued onto a mineral wool layer, provided on the outer side with longitudinal ventilated channels (Fig. 2). The cross-section of the ventilated channels is  $20 \text{ mm} \times 40 \text{ mm}$ , the separation between neighboring channels being  $62 \text{ mm}$ . The latter dimensions were chosen based on the heat-moisture analysis, whose results are reported below. The total thickness of the panel heat-insulating layer  $d$  varies depending on the particular panel application. The dimensions of a standard panel are  $3000 \text{ mm} \times 1190 \text{ mm}$ .

The panels are mounted on a newly constructed or renovated building wall with steel anchors (Fig. 1). In mounting the panels, in between them, horizontal gaps are left to be filled with mineral wool down to the bottom of ventilated channels; in this way, horizontal ventilation slits, covered from the outside with weather strips, are formed.

## 3. Thermophysical analysis

In construction and renovation of buildings, whose structural layer has a reduced thermal resistance  $R_0$ , there is a need to determine the thickness of a heat-insulating panel, providing for the reduced outer-wall thermal resistance

$$R_{\text{req}} = R_0 + R_p,$$

where  $R_p$  is the panel thermal resistance.

Using the computer program "Term 5" [22], allowing 2D simulation of building structures, we carried out thermal calculations of ventilated panels of various thicknesses. In the calculations, for the thermal conductivity of the mineral wool layer in the panels, a value  $0.042 \text{ W}/\text{m K}$ , typical of a wide range of mineral wool thermal insulators, was adopted. Data for one of the analyzed designs are shown in Fig. 2. From an analysis of the plots of  $R_p$  vs  $d$ , it follows that this dependence is linear in the interval  $80 \text{ mm} \leq d \leq 250 \text{ mm}$ ; this linear dependence can be presented as

$$R_p = 0.0238(d - 80) + 1.621$$

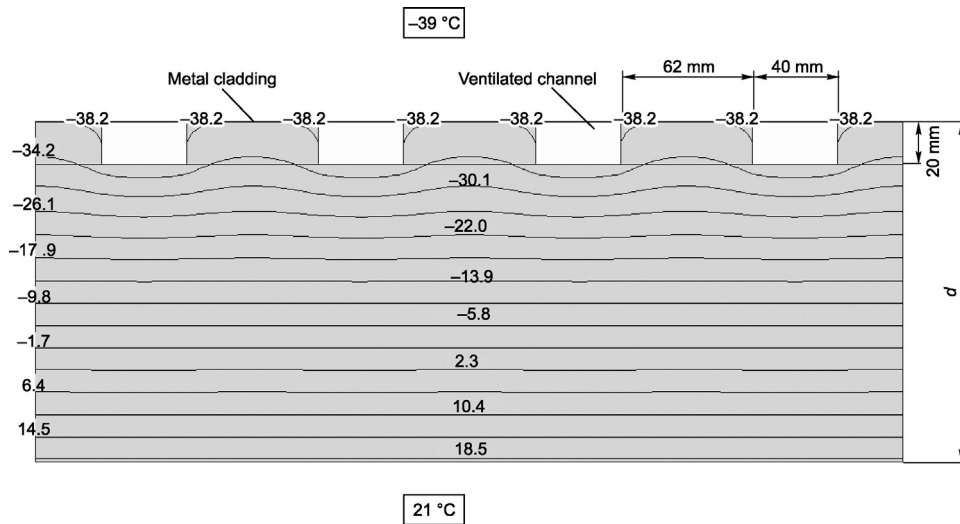


Fig. 2. Thermal data calculated for a 160-mm thick heat-insulating panel.

Further, we carried out thermal calculations of the reduced resistance to the transfer of heat for brick building walls with clay brick layer thicknesses 250-, 380-, and 640-mm ( $R_{red}^{250}$ ,  $R_{red}^{380}$ , and  $R_{red}^{640}$ , respectively) provided with external heat insulation, formed by ventilated panels of various thicknesses. The calculations were performed with the computer program “Term 5”, taking into account a 20-mm thick cement-sand plaster layer, covering the inner surface of the wall. In calculations of the reduced thermal resistances, the total coefficients of heat transfer from the outside and inside were adopted to equal respectively 23 and 8.7 W/m<sup>2</sup> K. These data can be generalized with the following dependences:

$$R_{red}^{640} = 0.0238(d - 80) + 2.722$$

From the results of thermal calculations, we were able to determine the recommended thicknesses of heat-insulating panels with ventilated channels for brick walls of various thicknesses on the condition of a 5–10% excess of the reduced thermal resistance of building walls, specified for Novosibirsk climatic conditions by Construction specifications and regulations [23]. The recommended thickness of heat-insulating panels for 250-, 380-, and 640-mm thick brick walls was found to be respectively 160, 150, and 140 mm.

Mounting of heat-insulating panels on a brick wall with metal anchors entails an additional heat loss, whose relative measure is given by the heat transfer performance uniformity factor;  $r = R_{red+} / R_{red}$ , where  $R_{red+}$  and  $R_{red}$  are the reduced thermal

$$R_{red}^{250} = 0.0238(d - 80) + 2.165$$

$$R_{red}^{380} = 0.0238(d - 80) + 2.351$$

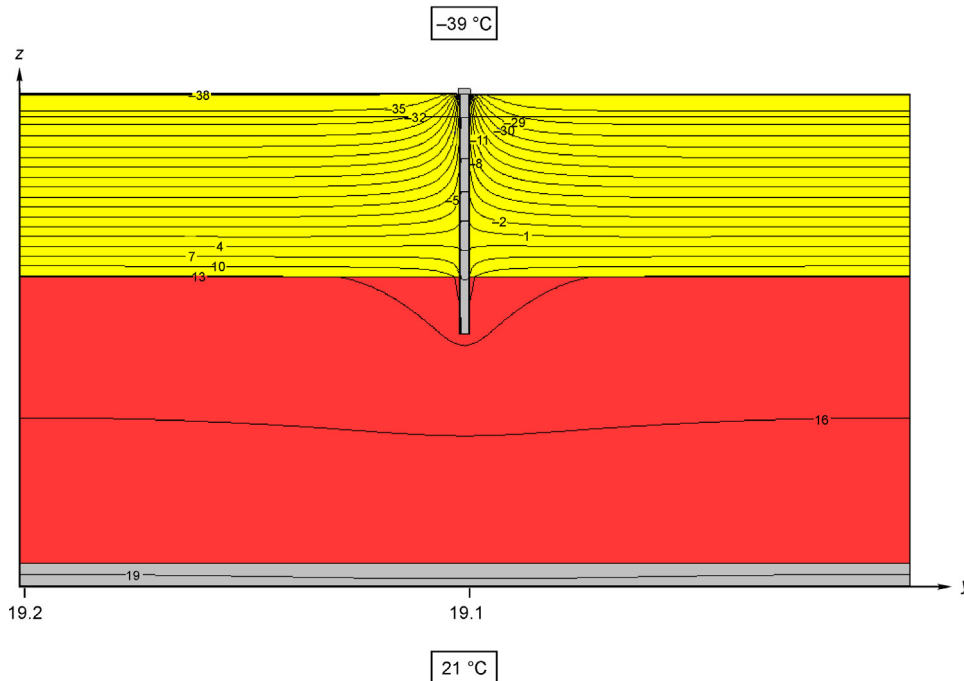
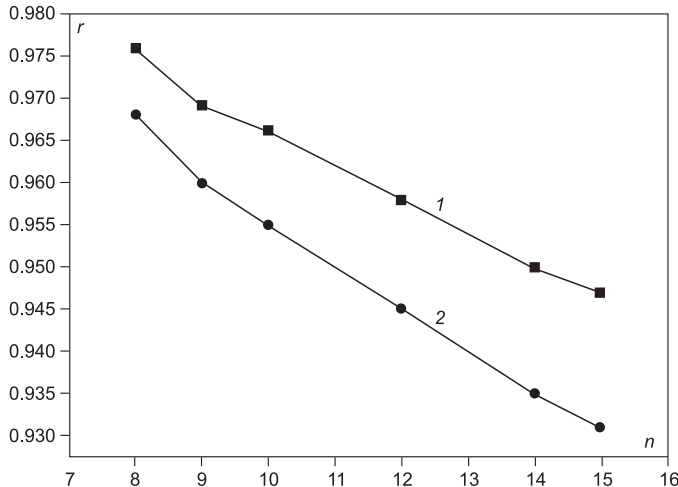


Fig. 3. Calculated distribution of temperature in the anchor plane for 250-mm thick brick wall and for 15 anchor/panel.

**Table 1**  
Properties of materials.

Material	Bulk density, kg/m <sup>3</sup>	Porosity, m <sup>3</sup> /m <sup>3</sup>	Spec heat capacity, J/kg K	Thermal conductivity, W/m <sup>2</sup> K	Water vapor diffusion resistance factor
Cement-sand plaster	1900	0.24	850	0.8	19
Clay brick masonry	1900	0.24	850	0.6	10
Mineral wool	110	0.95	850	0.042	3.3



**Fig. 4.** Heat transfer performance uniformity factors of thermally insulated brick wall for different numbers of mounting anchors per panel. 1 – 640-mm thick brick layer, 2 – 250-mm thick brick layer.

resistances of the building wall, determined with and without allowance for the anchors.

With the aim of determining the heat transfer performance uniformity factors of panel anchoring, we carried out thermal calculations for the newly constructed brick walls (brick layer thickness 250 mm, panel thickness 160 mm) and renovated brick walls (brick layer thickness 640 mm, panel thickness 140 mm). In the calculations, the inner surface of the brick walls was assumed to be covered by a 20-mm thick cement-sand plaster layer.

The calculations were performed using the specialized computer program HEAT 3.5, intended for 3D thermal calculations of building structural elements [24]. In the calculations, we treated the case of a standard 1.19 m × 3 m heat-insulating panel with ventilated channels, mounted on the brick wall with 8, 12, or 15 steel anchors of 8 mm diameter. The dimensions of the computational domain were defined by the panel area per one anchor. The indoor and outdoor air temperatures were assumed to be 21 °C and –39 °C, which case refers to the coldest five-day period in Novosibirsk [25].

By way of example, Fig. 3 shows the distribution of wall temperature in the anchor section over a 250-mm thick brick layer, heat-insulated with a panel of 160 mm thickness, fixed on the brick wall with 15 anchors. According to the calculated data, the inner-surface wall temperature at the place opposite to the anchor location was rather high, 19.1 °C, and differed by as little as 0.1 °C from the inner-surface wall temperature far from the anchor.

Using the calculated data, we have determined the heat transfer performance uniformity factors of panel anchoring for brick walls of 250 and 640 mm thicknesses for different numbers of anchors per panel (Fig. 4). The performed thermal calculations showed that the heat transfer performance uniformity factors for anchored panels with ventilated channels in the case of both newly constructed and renovated buildings fell in the range from 0.98 to 0.93, those values

being notably in excess of the heat transfer performance uniformity factors of traditional ventilated-facade designs [26].

#### 4. Moisture analysis

To identify the moisture state of walls in newly built or renovated buildings, thermally insulated with ventilated panels, we carried out a moisture analysis of two facade designs:

*Design 1.* A 250-mm thick clay brick wall of a new building is thermally insulated from the outside with 160-mm thick panels having ventilated channels.

*Design 2.* A 640-mm thick clay brick wall of a renovated building is thermally insulated from the outside with 140-mm thick panel having ventilated channels.

As a heat insulator in the panels, a mineral wool of 110 kg/m<sup>3</sup> density was used. The calculations were performed on the assumption that the inner wall surface was covered with a 20-mm thick cement-sand plaster layer.

In the calculation of both designs, identical boundary conditions were adopted. The indoor temperature and the relative air humidity were assumed to be respectively 21 °C and 55%. From the outside, the air temperature, the relative air humidity, and the incident solar radiation intensity were specified at 1-h step for a typical year close to the climatic conditions of Novosibirsk.

The calculations were performed for building walls oriented to the west. The coefficient of solar radiation absorption by the outer wall surface was taken equal to 0.4. The calculations were performed for a period of three years, starting from August 1.

The calculations were performed using the computer program “Wufi 2D-3” intended for 2D non-stationary heat–moisture calculations of building structures [27].

Properties of layer materials and their dependencies on temperature and humidity were taken from the library of materials properties of “Wufi 2D-3” program, and the basic materials properties, used in the calculations, are presented in Table 1.

Air humidity and temperature in the ventilated channels were taken for the calculations, based on the parameters of the outdoor air, that is proved to be reasonable according to further estimates of air velocities in the channels, moisture flows through the walls and due to the horizontal slits present every 3 m over the facade height.

In the calculations, we took into account the dependence of moisture storage capacity on relative humidity of all considered materials, including the mineral wool.

The algorithm of the program is based on numerical solution of the equation system, involving the enthalpy conservation equation (1) and the moisture-mass conservation equation (2). The specified boundary conditions are certain values of heat-flux density (3) and moisture flow density (4) [28]

$$\frac{\partial H}{\partial t} \frac{\partial t}{\partial \tau} = \frac{\partial}{\partial x} \left( \lambda_x \frac{\partial t}{\partial x} \right) + \frac{\partial}{\partial y} \left( \lambda_y \frac{\partial t}{\partial y} \right) + h \frac{\partial}{\partial x} \left( \mu_x \frac{\partial \varphi P_{\text{sat}}}{\partial x} \right) + h \frac{\partial}{\partial y} \left( \mu_y \frac{\partial \varphi P_{\text{sat}}}{\partial y} \right) \quad (1)$$

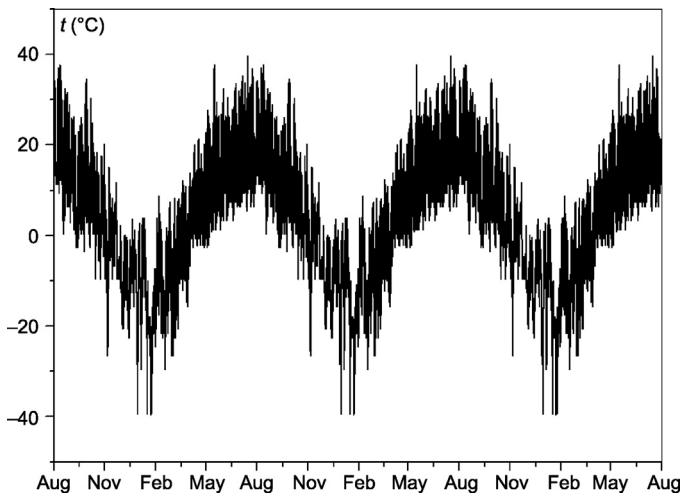


Fig. 5. Variation of outer-surface wall temperature (250-mm thick brick layer).

$$\frac{\partial W_V}{\partial \varphi} \frac{\partial \varphi}{\partial \tau} = \frac{\partial}{\partial x} \left( D_x \frac{\partial W_V}{\partial \varphi} \frac{\partial \varphi}{\partial x} + \mu_x \frac{\partial \varphi P_{sat}}{\partial x} \right) + \frac{\partial}{\partial y} \left( D_y \frac{\partial W_V}{\partial \varphi} \frac{\partial \varphi}{\partial y} + \mu_y \frac{\partial \varphi P_{sat}}{\partial y} \right) \quad (2)$$

$$q = \alpha(t_{air} - t_b) + q_s k \quad (3)$$

$$q_m = \beta(P_{air} - P_b) \quad (4)$$

4.1. Moisture state of a new building wall

The initial relative humidity of the brick and plaster layers in the newly built building wall was assumed substantial, equal to the sorption humidity of involved materials at 80% relative air humidity.

In calculations with outer-wall surface temperature lowering in winter months (see Fig. 5), the density of the heat flux through the wall showed an increase with the highest values running into 10 W/m<sup>2</sup> (Fig. 6).

Fig. 7 shows the variation of the average relative mass humidity of the panel mineral wool layer. According to the calculated data, in the first-year winter season after the wall was built, the

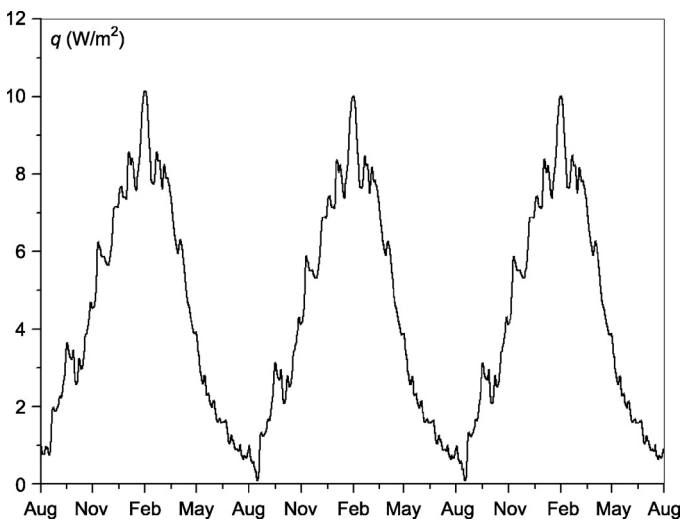


Fig. 6. Variation of heat-flux density on the inner wall surface (250-mm thick brick layer).

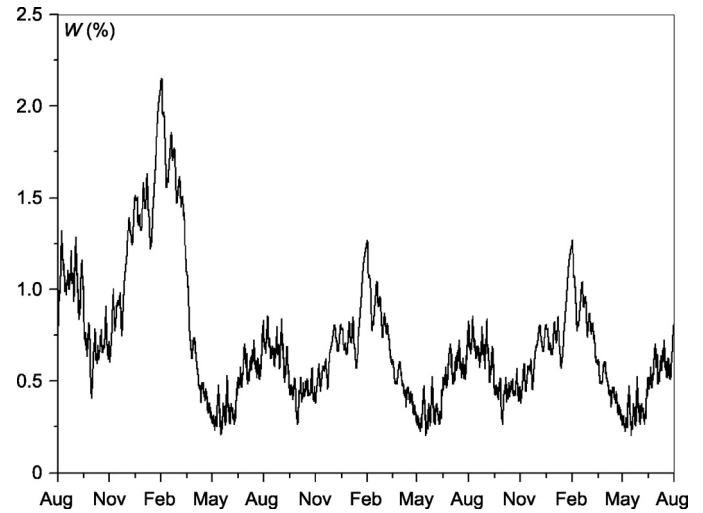


Fig. 7. Mean relative humidity of the mineral wool layer (250-mm thick brick layer).

humidity was somewhat greater than 2% due to the enhanced moisture content of the brick layer, and afterwards the humidity showed a decrease. In subsequent years in the winter time, the humidity increased to 1.5%. Such an increase of the humidity of the mineral wool layer can be considered insignificant, only weakly affecting the thermal insulating properties of the heat-insulation material. Thus, as calculations showed, the heat-insulation material in a panel with ventilated channels was in a rather dry state with no danger of fungus growth. This is evident from the data of Fig. 8; in this figure, the dots indicate the hydrothermal conditions

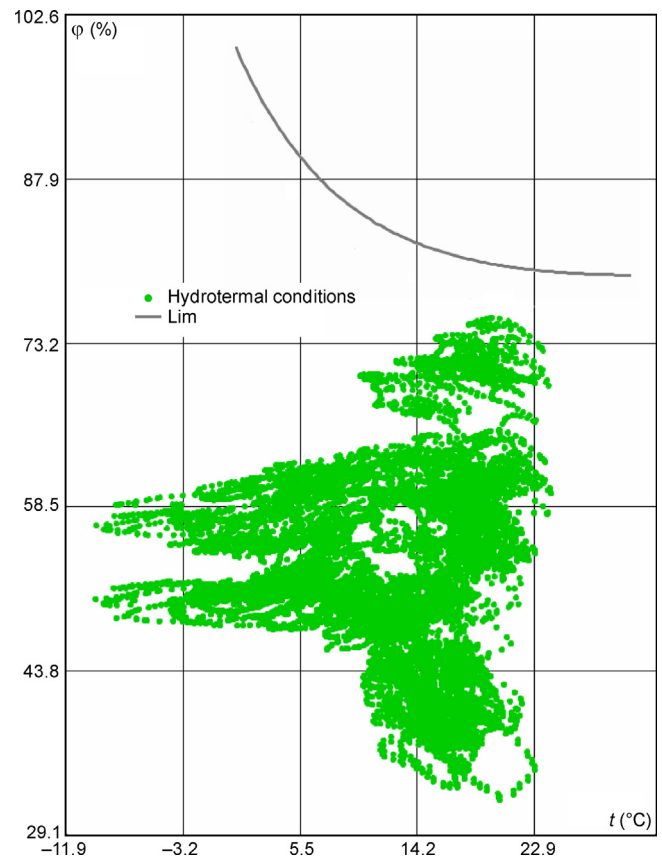


Fig. 8. Hydrothermal conditions in the heat-insulator layer (250-mm thick brick layer).

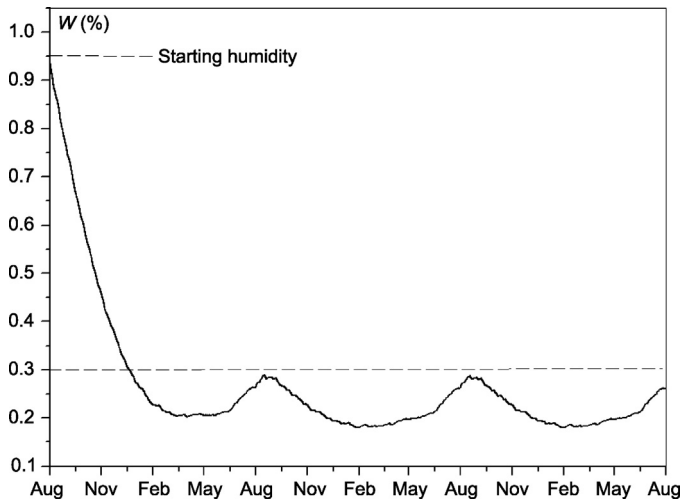


Fig. 9. Mean relative humidity of the brick layer (250-mm thick brick layer).

in the heat-insulation material at different times. The same figure shows the hydrothermal curve, over which the appearance of fungi becomes possible in the heat-insulation material.

As it is evident from calculations, the relative humidity of the brick layer showed a sharp decrease during the first year after the construction of the building; later this humidity was at a level of 0.2%, showing insignificant rises to 0.3% in the periods from the end of summer to the beginning of autumn (Fig. 9). Note that, on the whole, the humidity level of the brick layer was rather low.

Fig. 10 shows distribution of average volume humidity in the brickwork and in the heat-insulating layer of the panel in the 3rd year after the construction completion in August, when there were maximal humidity increase in the brick masonry and some increase of humidity in the heat-insulating layer. According to the calculated results, humidity of brick masonry both in August and February decreased from the internal to external surface; and over its thickness, humidity in February was lower than in August. In panel heat-insulation layer, humidity of the outer layers in the considered months was higher than in the internal ones. In February, it was due

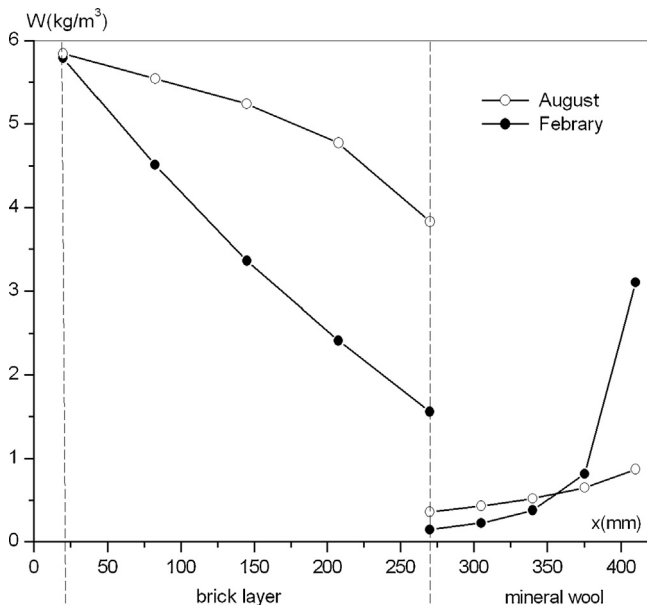


Fig. 10. Month average humidity distribution (250-mm thick brick layer).

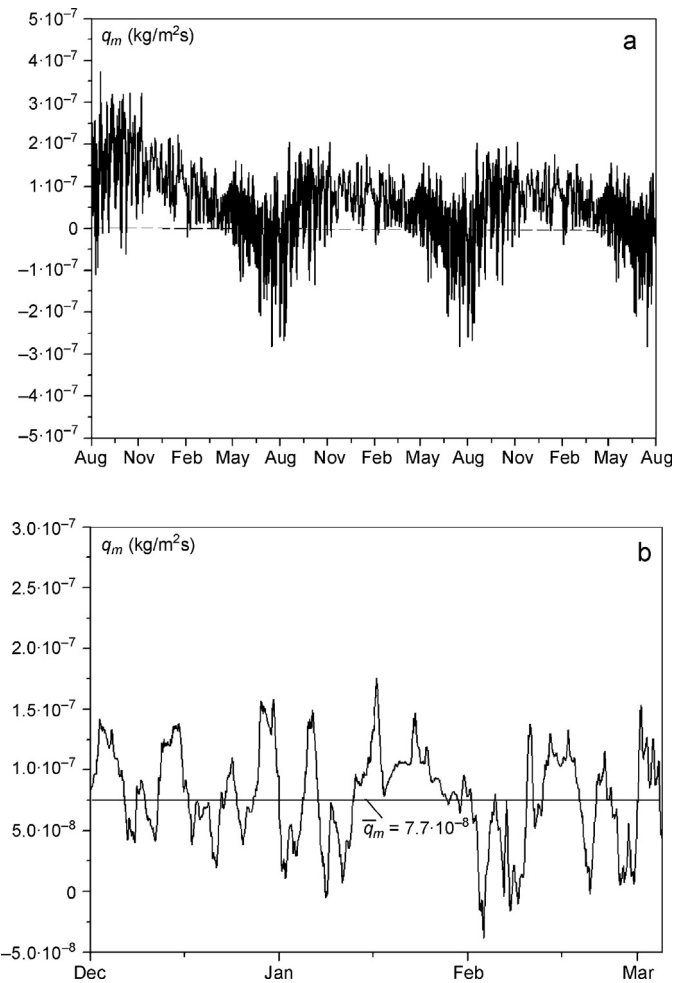


Fig. 11. Moisture diffusion flux density at the brick layer/heat insulator interface: (a) over a three-year period, (b) during the winter season (250-mm thick brick layer).

to the lower temperature of the outer layers, and in August – due to the higher humidity of the outer air at its rather high temperature.

As a result of calculations, the density and the direction of the moisture diffusion flux across the brick layer/heat-insulation layer interface were determined (Fig. 11 a). An analysis of the data shows that in winter, the moisture flux is positive, directed from the brick to thermal-insulation layer, and in summer, it is predominantly negative, directed from the thermal-insulation layer into the brick wall.

To judge whether the ventilated channels will be capable or not of providing for the necessary removal of the moisture, accumulated in the thermal-insulation material, we determined the average density of the diffusion flux of moisture during the winter months,  $\bar{q}_m = 7.7 \times 10^{-8}$  kg/m<sup>2</sup>s (Fig. 11b). We performed a gas dynamics analysis of the ventilated channels in January for the mean outdoor temperature  $-18.8$  °C and relative air humidity of 80%, the latter values being typical of the Novosibirsk climatic conditions. The evaluated velocity of the air flow in the channels was 0.2 m/s. The calculations showed that, under the conditions with inter-storey air inlet and outlet openings into a ventilation channel, each ventilated channel was capable of removing moisture at a rate of up to  $0.3 \times 10^{-7}$  kg/s, the necessary rate of moisture removal being  $0.2 \times 10^{-7}$  kg/s.

Thus, the calculations showed that, with properly organized inter-storey air openings into the ventilated channels, the examined configuration of the ventilated channels provides for efficient removal of moisture out of the heat-insulation material.

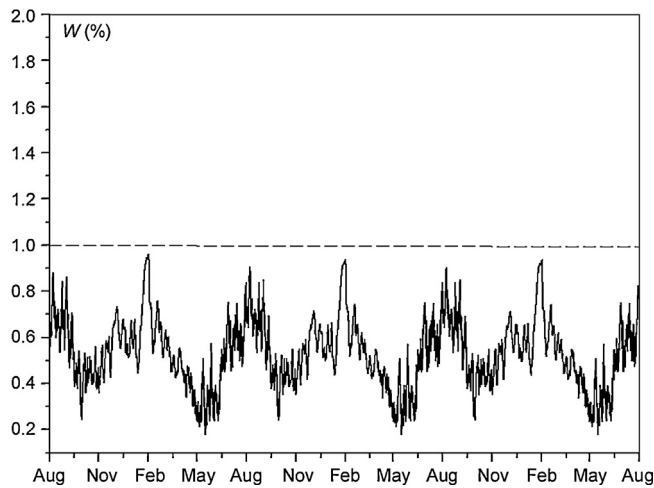


Fig. 12. Mean relative humidity of the mineral wool layer (640-mm thick brick layer).

4.2. Moisture state of a renovated building wall

A 640 mm thick brick wall in a renovated building was assumed thermally insulated with 140-mm thick panels with ventilated channels, installed using no wet processes; that is why in the calculations, the initial moisture content of the brick and plaster layers was taken equal to the sorption humidity of the materials at 50% air humidity.

According to the calculated data, no accumulation of moisture in the mineral wool layer of the panel occurred during the annular cycle, with just cyclic oscillations of mean relative humidity at the end of summer and in the winter season being observed (here, the relative humidity varied within 1% (Fig. 12)). During the whole calculated period, the mineral wool remained rather dry and, as hydrothermal calculations showed, no danger of fungi formation and growth occurred in the heat-insulation layer.

The calculated data on the variation of brick layer humidity on average and over component layers are shown in Fig. 13. From these data it follows that the mean moisture content of the brick wall is rather low, with an insignificant rise of material humidity at the end of summer and the beginning of autumn (Fig. 13a). The analysis of the distribution of the moisture content over the component brick-wall layers reveals the fact that the most humid one is the inner brick-wall layer, while the largest amplitude of the annular oscillations of material humidity is observed in the outer layer (Fig. 13b).

Distribution of average volume humidity for the month in the brick and heat insulating layer of the wall in August and February of the 3rd year is shown in Fig. 14.

Similarly to the earlier considered calculation option for the wall with a brick layer of 250 mm thickness (Fig. 10), humidity distribution in heat insulation was similar to humidity increase from to the outer surface due to the abovementioned reasons. In the internal part of the brick masonry, humidity in February turned out to be higher than in August, and for the wall with 250 mm brick masonry – vice versa; that was obviously bound with the lag effect of moisture transfer processes in the thicker brick layers.

We also performed calculations of the variation of the moisture diffusion flux across the brick layer/heat-insulator layer interface. The calculation showed that, similar to the case of design 1, in winter, the moisture flow is directed out of the brick layer into the heat insulator, and in summer, predominantly in the opposite direction, out of the heat insulator into the brick wall (Fig. 15a).

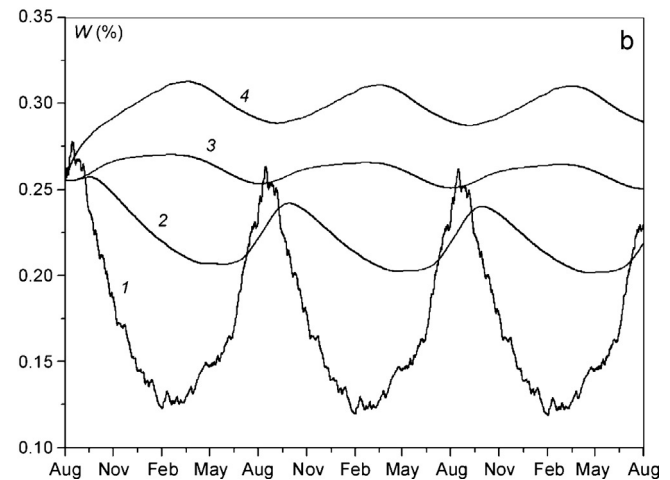
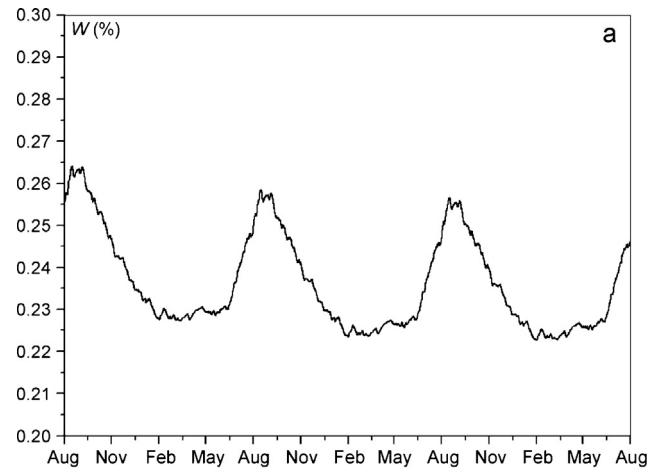


Fig. 13. Mean relative humidity of the brick layer (a) in the whole brick layer, (b) in different component layers of the brick wall: Digits 1–4 enumerate the component layers from the outside to inside (640-mm thick brick layer).

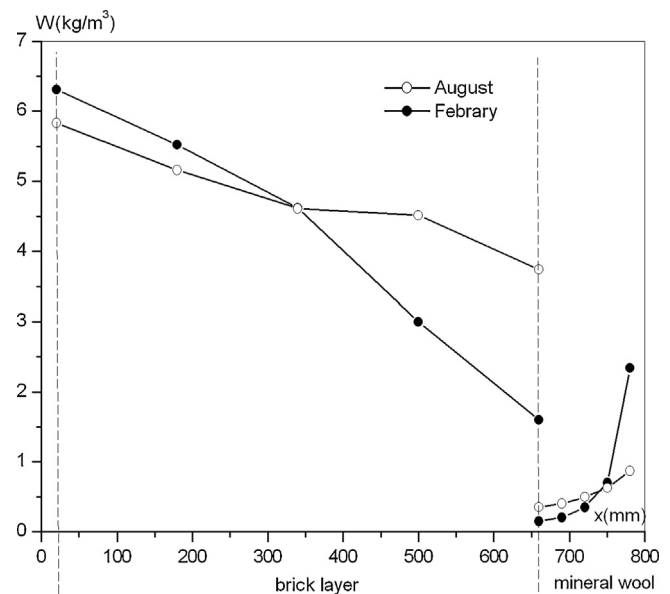
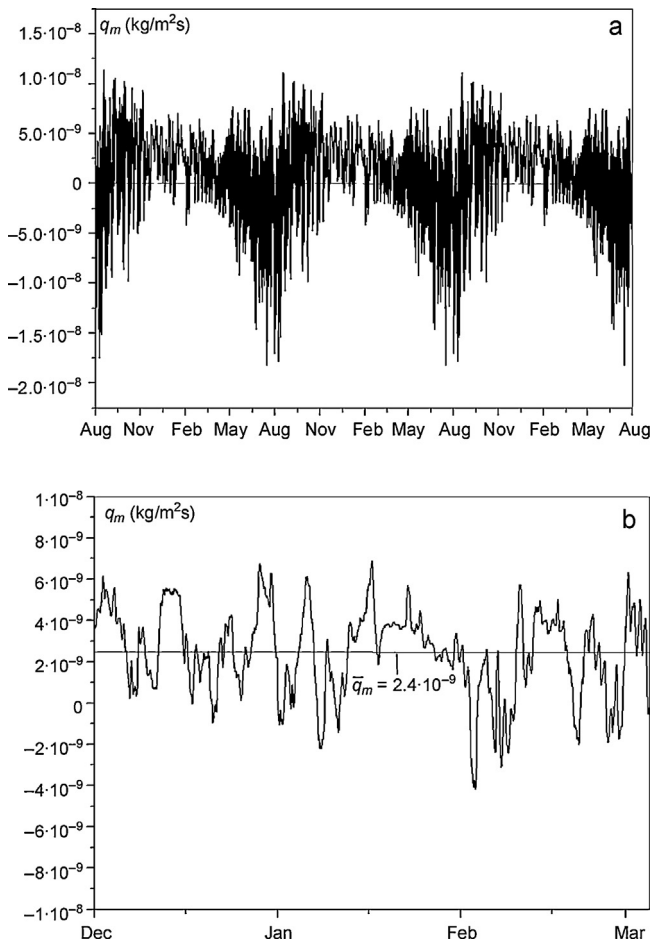


Fig. 14. Month average humidity distribution (250-mm thick brick layer).



**Fig. 15.** Moisture diffusion flux at the brick layer/heat insulator interface, (a) over a three-year period, (b) during the winter season (640-mm thick brick layer).

According to the calculations, in winter season, the mean moisture diffusion flux across the brick wall/heat insulator interface was  $2.4 \times 10^{-9} \text{ kg/m}^2 \text{ s}$  (Fig. 15b). The latter value is more than three times lower than the same quantity for a newly constructed building (design 1), so that the ventilated channels in the panels are quite capable of ensuring an efficient removal of this moisture.

It should be noted that in these calculations, effect of solar radiation, falling on the outer wall surface, was considered only through the temperature increase on the external surface of the heat-insulating layer beyond the ventilation channels; therefore according to the calculated results, influence of solar radiation on materials humidity was weak. In real situation, solar radiation will also heat the outer walls of the ventilation channels, that will in turn increase air temperature in the ventilation channels; and this will lead to the decrease in relative humidity and growth of air velocity in the ventilation channels. Consideration of these processes will result in even lower humidity of construction and heat insulation materials of the walls compared to the ones obtained in the calculations.

#### 4.3. Practical implementation and results of inspections

Presently, the thermal insulating facade systems based on the ventilated channels panels were installed on more than ten new and renovated buildings in Novosibirsk and Novosibirsk Region; two renovated buildings are shown in the photos of Fig. 16.

The use of a broad assortment of decorative coatings allows realization of a multitude of design solutions in the thermal insulation



**Fig. 16.** A building thermally insulated with the ventilated panels: (a) a dwelling house, (b) an office block.

of buildings with the heat-insulating panels. The experience gained in installation of the new facade system on newly constructed and renovated buildings has proved the possibility of performing efficient, good-quality installation works.

The thermal imaging inspections of several buildings performed in the winter time have confirmed the high thermal performance of the new facade system. Some results of thermal imaging study of the three-floored building with the outer walls, made of clay bricks with the thickness of 510 mm, partially covered by the panels, are shown in Fig. 17 as an example of efficient application of the panels with ventilated channels, used for heat insulation of previously constructed buildings. The outside air temperature at investigation was  $-14.5^\circ\text{C}$ . The picture and thermogram of the outer corner of the building, where one wall is covered by the panels and another is free of them, are shown in Fig. 17a and b. According to investigation results, the temperature of the outer surface of the panels is  $3.5\text{--}4^\circ\text{C}$  lower than the temperature of the outer surface of brick walls, which are not covered by the panels. This proves a significant (several times) decrease in the heat losses through the walls, covered by heat insulating panels with ventilated channels. The similar conclusion is made by the results of the indoor thermal imaging. At the inner air temperature of  $26\text{--}27^\circ\text{C}$  the temperature of the inner surface of the outer wall in the room with a wall covered outside by the panels (Fig. 17c) is more than  $4^\circ\text{C}$  higher than the temperature of the inner surface in the room without heat insulation of the outer wall (Fig. 17d). Thus, thermal imaging confirms high efficiency of the panels with ventilated channels used for heat insulation of reconstructed buildings.

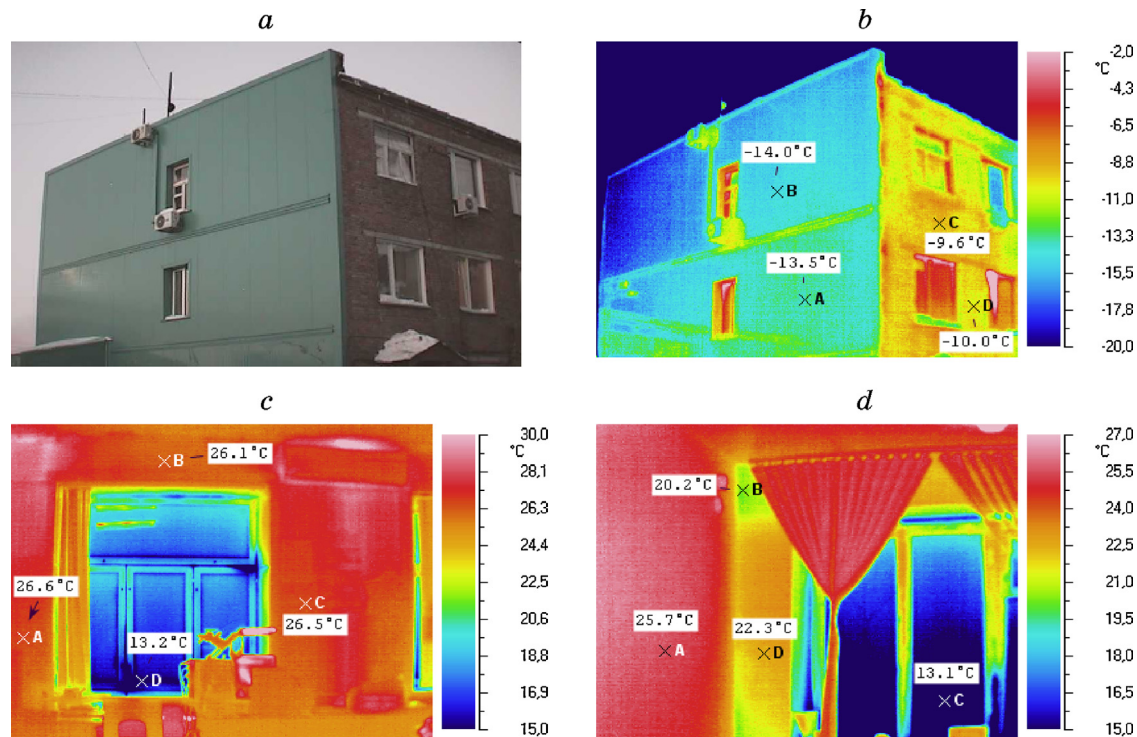


Fig. 17. Results of thermal imaging study of outer walls of the building: (a) the picture of the outer corner of the building with one heat insulated surface; (b) thermogram of the outer corner; (c) thermogram of the inner surface of the wall with heat insulation; (d) thermogram of the inner surface of the wall without heat insulation.

## 5. Conclusions

We have proposed and implemented a new facade system based on factory-produced heat-insulating panels with ventilated channels for thermal insulating for newly constructed and renovated buildings.

A numerical thermophysical analysis was performed to determine the thermal resistance of panels versus panel thickness. Reduced thermal resistances of brick walls of various thicknesses thermally insulated with heat-insulating panels with ventilated channels were also determined.

The thermal calculations showed that, due to the applied panel anchoring method using steel anchors, the heat transfer performance uniformity factors of the new facade thermal insulating system can be made varying in the range from 0.98 to 0.93, these values being well in excess of the similar factors for traditional ventilated-facade designs.

The performed thermofluid-dynamics analysis showed that, for newly constructed and renovated brick buildings, the facade systems based on the panels with ventilated channels of proposed configuration can be used in building construction, with the brick and thermal-insulation layers in the panels remaining rather dry in a state complying with technical specifications. No moisture condensation and accumulation occurs in the facade system with due organization of inter-storey air openings into ventilation channels. The thermal imaging inspections have confirmed the high thermal performance of the new facade system.

## References

- [1] C. Suarez, P. Joubertb, J.L. Molinaa, F.J. Sanchezca, Heat transfer and mass flow correlations for ventilated facades, *Energy and Buildings* 43 (2011) 3696–3703.
- [2] F. Patania, A. Gagliano, F. Nocera, A. Ferlito, A. Galesi, Thermofluid-dynamic analysis of ventilated facades, *Energy and Buildings* 42 (2010) 1148–1155.
- [3] C. Balocco, A simple model to study ventilated facades energy performance, *Energy and Buildings* 34 (2002) 469–475.
- [4] G. Gan, Simulation of buoyancy-induced flow in open cavities for natural ventilation, *Energy and Buildings* 38 (2006) 410–420.
- [5] A. Pappas, Z. Zhai, Numerical investigation on thermal performance and correlation of double skin facade with buoyancy-driven airflow, *Energy and Buildings* 40 (2007) 466–475.
- [6] C. Suarez, P. Joubertb, J.L. Molinaa, F.J. Sanchezca, Heat transfer and mass flow correlations for ventilated facades, *Energy and Buildings* 43 (2011) 3696–3703.
- [7] A. Bar-Cohen, W.M. Rohsenow, Thermally optimum spacing of vertical, natural convection cooled, parallel plates, *ASME Journal of Heat Transfer* 106 (1984) 116–123.
- [8] W.M. Rohsenow, J.P. Hartnett, Y.I. Cho, *Handbook of Heat Transfer*, McGraw-Hill, New York, 1998.
- [9] E.M. Sparrow, G.M. Chrysler, L.F. Azevedo, Observed flow reversal and measured-predicted Nusselt numbers for natural convection in a one-sided heated vertical channel, *ASME Journal of Heat Transfer* 106 (1984) 325–332.
- [10] T.F. Ayinde, S.A.M. Said, M.A. Habib, Experimental investigation of turbulent natural convection flow in a channel, *Heat and Mass Transfer* 42 (2006) 169–177.
- [11] V. Serra, F. Zanghirella, M. Perino, Experimental evaluation of a climate facade: energy efficiency and thermal comfort performance, *Energy and Buildings* 42 (2010) 50–62.
- [12] C. Marinoscia, P.A. Strachanb, G. Semprinia, G.L. Morinia, Empirical validation and modelling of a naturally ventilated rainscreen facade building, *Energy and Buildings* 43 (2011) 853–863.
- [13] P. Seferis, P. Strachana, A. Dimoudib, A. Androutsopoulosc, Investigation of the performance of a ventilated wall, *Energy and Buildings* 43 (2011) 2167–2178.
- [14] M. Ciampi, F. Leccese, G. Tuoni, Ventilating facades energy performance in summer cooling of buildings, *Solar Energy* 75 (2003) 491–502.
- [15] A. Fallahi, F. Haghighat, H. Elsadi, Energy performance assessment of double-skin facade with thermal mass, *Energy and Buildings* 42 (2010) 1499–1509.
- [16] R. Fulliotto, F. Cambuli, N. Mandas, N. Bacchin, G. Manara, Q. Chen, Experimental and numerical analysis of heat transfer and airflow on an interactive building facade, *Energy and Buildings* 42 (2010) 23–28.
- [17] J.A. Clarke, P.A. Strachan, Simulation of conventional and renewable building energy systems, *Renewable Energy* 5 (1994) 1178–1189.
- [18] L. Mei, D.G. Infield, U. Eicker, V. Fux, Thermal modelling of a building with an integrated ventilated PV facade, *Energy and Buildings* 35 (2003) 605–617.
- [19] C. Sanjuana, M.J. Suarez, M. Gonzalez, J. Pistono, E. Blanco, Energy performance of an open-joint ventilated facade compared with a conventional sealed cavity facade, *Solar Energy* 85 (2011) 1851–1863.
- [20] M. Jerman, R. Cerny, Effect of moisture content on heat and moisture transport and storage properties of thermal insulation materials, *Energy and Buildings* 53 (2012) 39–46.
- [21] Patent (RU) for Useful Model No. 94597, Wall panel for cladding and warming of building (May 27, 2010).

- [22] TERM 5.2/WINDOW 5.2 NFRC Simulation Manual, Lawrence Berkeley National Laboratory, 2006.
- [23] Construction specifications and regulations 23-02-2003, Thermal Protection of Buildings, Gosstroii Rossii, Moscow, 2004.
- [24] T. Blomberg, HEAT 3 a PC- program for heat transfer in three dimensions., Manual with brief theory and examples, Lund-Gotheenborg Group for Computational Building Physics Department of Building Physics, Lund University Building Technology Group, Massachusetts Institute of Technology (2001).
- [25] Construction specifications and regulations 23-01-99\*, Building Climatology, Gosstroii Rossii, Moscow, 2000.
- [26] V.G. Gagarin, V.V. Kozlov, E.Yu. Tsykanovskii, Thermal protection of facades with an air cavity, *Ventilyatsiya, Otoplenie, Konditsionirovanie vozdukha, Teplosnabzhenie i Stroitel'naya Teplofizika* 3 (2004) 20–26.
- [27] D. Zirkelbach, Th. Schmidt, H.M. Kunzel, M. Kehrer, Ch. Bludau, *WIFI 2D Installation and Introduction*, Fraunhofer Institute of Building Physics, 2007.
- [28] H.M. Kunzel, *Simultaneous heat and moisture transport in building components* (Ph.D. thesis), Fraunhofer Institute of Building Physics, Germany, 1995.